Gaussian Process Interpolation for Uncertainty Estimation in Image Registration

Loïc TETREL
McGill / Ecole de technologie supérieure
ECSE-626
loic.tetrel@mail.mcgill.ca

Abstract

Resampling a grid is an inherent step of intensity-based image registration to evaluate similarity between pixel values at the same position. However, interpolation error varies among grid point and must be took into account in the similarity measure. We employ a bayesian regression with a gaussian process prior over images to predict a gaussian shape function with mean corresponding to resampled values and covariance is the uncertainty. We show that the proposed approach increases registration accuracy for MRI-T1 images. Moreover it is easily integrated to existing registration methods.

1. Introduction

Image registration is an inherent field of medical imaging to align images. It helps clinicians to visualize images under the same context, or to fuse information from different modalities. Such alignement can be found using two types of registration : feature-based and intensity-based. With feature-based methods, we want to find the same key-points in two images and use them to realign or register the images. Intensity-based methods consist in evaluating the similarity between pixel intensities at the same position. By an iterative procedure, we want to find the optimal transformation $T(\mathbf{x})$ that maximizes similarity S between the fixed image $I_F(\mathbf{x})$ and the tranformed moving image $I_M(T(\mathbf{x}))$:

$$\hat{T} = \underset{T}{\operatorname{argmax}} S(I_F(\mathbf{x}), I_M(T(\mathbf{x}))) \quad (1)$$

The computation of the operation at eq. 1 needs to resample images into the same grid. The resampling operation consists in first interpolating the pixel of the image to have values for all the positions, and after taking samples at the wanted positions to extract the pixel values.

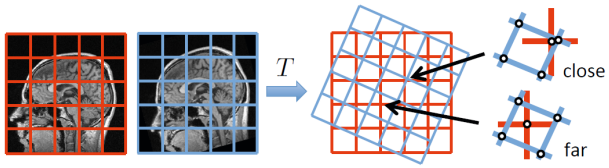

Figure 1. Moving (blue) and fixed (red) images. The interpolation uncertainty varies among grid points after transformation. Above the uncertainty is low because neighbouring points are close in contrary to below where points are far. Extracted from [14].

Interpolation was first used to increase the poor image resolution in the past. But more recently it has been shown that interpolating the image's pixels can help to have a more accurate measure when we want to find the pic of similarity [4]. Many interpolation methods have been used for image registration like nearest neighbour [9], cubic interpolation [5] or spline interpolation [12]. None of these interpolators are closed to the optimal *sinc* interpolator with bandpass between Nyquist frequency [13]. Gaussian Process (also called Kriging in geo statistics) is the interpolator that is the closest to the optimal interpolator [11].

One major problem is that interpolation uncertainty varies among the grid. The Fig. 1 shows two examples where the uncertainty is respectively low and high. This error causes artefacts [1] and bias the registration result, that is why it is necessary to take into account uncertainty in the registration process.

To have accurate interpolation with prediction of error, a bayesian regression is proposed in this paper. The transformed grid values are the observations and the prediction result in resampled values on the fixed grid. Assuming a $\mathcal{GP}$ prior over images and gaussian noise on the observations, the prediction is a multivariate gaussian with mean corresponding to resampled values and covariance is the uncertainty (sec. 2.1).

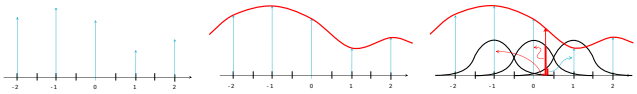

Figure 2. Process of resampling the grid points of transformed moving image $T(\Omega_{I_M})$ (blue) into the fixed image Ω_{I_F} (red) in 1D. From left to right : Sampled values $T(\Omega_{I_M})$, interpolation of $T(\Omega_{I_M})$ and one resampled value I_M^*.

This lead to a new similarity measure that takes into account the uncertainty of the interpolation (sec. 2.2). The results of the proposed approach are discussed in sec. 3, finally sec. 4 summarizes the contribution with the future perspectives.

2. Method

The goal is to find the rigid transformation $T(\mathbf{x})$ that transform the grid Ω_{I_M} of the moving image I_M into the grid Ω_{I_F} of the fixed image I_F. Resampling the transformed moving grid $T(\Omega_{I_M})$ at the points of the fixed grid Ω_{I_F} is necessary to compare the similarity of the pixel values of the two images. The resampling process of $T(\Omega_{I_M})$ consist in interpolating $T(\Omega_{I_M})$ samples to construct it continuous version. After we take samples at the position of Ω_{I_F} to have values of transformed moving image $I_M(T(\Omega_{I_M}))$ at the position of Ω_{I_F} (Fig. 2). From the prediction of resampled values, we develop a generative model for the registration which take into account uncertainty of the interpolation.

2.1. Gaussian Process interpolation

Gaussian process is used to obtain the interpolator with uncertainty estimates. "*A Gaussian Process is a stochastic process consisting of an infinite collection of random variables, where any finite subset has a multivariate Gaussian distribution [10]. A Gaussian Process* $\mathcal{GP}(m(\mathbf{x}), k(\mathbf{x}, \mathbf{x}'))$*, is entirely characterized by the mean* $m(\mathbf{x})$ *and covariance* $k(\mathbf{x}, \mathbf{x}')$ *functions.*" (Extracted from [14]).

We predict the resampled moving image I_M^* on the grid $X^* = \Omega_{I_F}$ using the moving image I_M on the transformed moving grid $X = T(\Omega_{I_M})$. We make the common asumption of a zero mean function [10] leading to the prior over resampeld value $I_M^* \sim \mathcal{GP}(0, k)$. Assuming a gaussian noise on the observations $\mathcal{N}(0, \sigma^2_{I_M})$ the predicted distribution of the resampled values is gaussian [14]:

$$p(I_M^*|I_M; X, X^*) = \mathcal{N}(\mu^*_{I_M}, \Sigma^*_{I_M}) \tag{2}$$

With mean, covariance and kernel defined as

$$\mu^*_{I_M} = k(X^*, X).[k(X, X) + \sigma^2_{I_M}\mathbf{I}]^{-1}.I_M \tag{3}$$

$$\Sigma^*_{I_M} = k(X^*, X^*) - \frac{\mu^*_{I_M}}{I_M}.k(X, X^*) \tag{4}$$

$$k(\mathbf{x}, \mathbf{x}') = \exp(-\frac{\|\mathbf{x} - \mathbf{x}'^2\|}{2l^2}) \tag{5}$$

The use of squared exponential kernel is common with $\mathcal{GP}$ [10] because it captures the smooth relation between neighbours pixels. "*The squared exponential kernel corresponds to a Bayesian linear regression model with an infinite number of Gaussian-shaped basis function.*" (Extracted from [14]). The lengthscale l is related to the bandwith of the kernel and has to be choose carefully to improve accuracy.

2.2. Generative model for registration with Gaussian Process interpolation

A new generative model is designed to create a new similarity measure which take into account uncertainty of resampling. The inputs of this generative model are the fixed image I_F and moving image I_M respectively with gaussian noise $\mathcal{N}(0, \sigma^2_{I_F})$ and $\mathcal{N}(0, \sigma^2_{I_M})$. The estimation of the optimal transformation $\hat{T}$ is performed with maximum likelihood estimation on the joint distribution $p(I_F, I_M)$ [14] leading to :

$$\hat{T} = \underset{T}{\operatorname{argmax}}\ p(I_F, I_M) \tag{6}$$

The resampled values I_M^* is a latent random variable and has to be taken into account in the joint distribution :

$$p(I_F, I_M, I_M^*) = p(I_M^*|I_M).p(I_F|I_M^*) \tag{7}$$

The joint distribution of eq. 7 is the product of the posterior $p(I_M^*|I_M)$ (the predicted resampled values from sec. 2.1), and the likelihood $p(I_F|I_M^*)$. Assuming an independent and identically distributed gaussian noise on the pixel values, the likelihood is gaussian $p(I_F|I_M^*) \sim \mathcal{N}(I_M^*, \sigma^2_{I_F}\mathbf{I})$. To extract the similarity between I_F and I_M, we marginalize the joint distribution $p(I_F, I_M, I_M^*)$ over the latent random variable I_M^* [14]:

$$
\begin{aligned}
p(I_F, I_M) &= \int p(I_F, I_M, I_M^*)\ dI_M^* \\
&= \int p(I_M^*|I_M).p(I_F|I_M^*)\ dI_M^* \\
&= \int \mathcal{N}(I_M^*; \mu_{I_M}^*, \Sigma_{I_M}^*). \\
&\quad \mathcal{N}(I_F; {I_M}^*, \sigma_{I_F}^2 \mathbf{I})\ dI_M^* \\
&= \mathcal{N}(I_F; \mu_{I_M}^*, \Sigma_{I_M}^* + \sigma_{I_F}^2 \mathbf{I})
\end{aligned} \tag{8}
$$

For computation purpose, we maximized the log-likelihood function instead of the likelihood, then the function becomes [14]:

$$
\begin{aligned}
\log p(I_F, I_M) &= \log\left((2\pi)^{-\frac{k}{2}}|\Sigma|^{-\frac{1}{2}}\right) - \\
&\quad \tfrac{1}{2}(I_F - \mu_{I_M}^*)^t \Sigma^{-1}(I_F - \mu_{I_M}^*)
\end{aligned} \tag{9}
$$

with the covariance

$$
\Sigma = \Sigma_{I_M}^* + \sigma_{I_F}^2 \mathbf{I} \tag{10}
$$

The new similarity measure $\log p(I_F, I_M)$ for registration now takes into account the interpolation uncertainty Σ. This similarity is close to the Mahalanobis distance [7] because the joint distribution of $p(I_F, I_M)$ is a multivariate gaussian.

3. Experimentation

3.1. Data acquisition

The experiments were performed using MATLAB® 2015b software and a UNIX system with a processor Intel® Xeon(R) CPU E3-1230 v3 @ 3.30GHz x 8 and 8GB RAM. The database consist of one 3D MRI-T1 brain volume acquired from one patent in RIRE dataset [3] with pixel resolution at 1.25mm. We selected randomly one axial slice and downsampled the image by a factor of 5 in one random direction to simulate common 2D anisotropic image in clinical context. An arbitrary regular grid of size 32×32 with 10mm spacing between points was used on the fixed image to create the moving image. After a grid of the same size 32×32 was applied on the moving image for the registration process (Fig. 3). We constrained our problem to rigid transformation defined by the homogeneous matrix :

$$
T(\mathbf{x}) = \begin{bmatrix} R(\mathbf{x}) & t(\mathbf{x}) \\ 0 & 1 \end{bmatrix}
$$

with rotation $R(\mathbf{x})$ but without translation $t(\mathbf{x}) = [0\ 0]$. Examples of images are shown in Fig. 4.

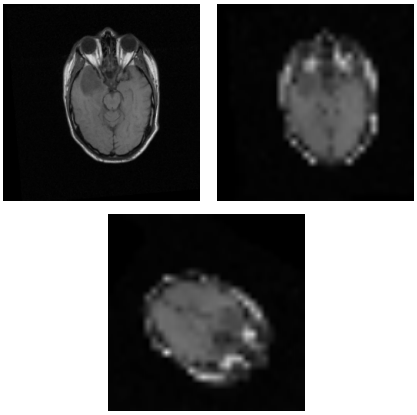

Figure 4. (Top) Fixed image and downsampling in x direction by 5. (Bottom) Moving image with rotation $\theta = -126.05°$.

3.2. Resampling and registration results

For experimentation, we set the gaussian variances $\sigma_{I_M}^2 = \sigma_{I_F}^2 = 0.01$ to simulate the noise on images. The lengthscale l of the covariance function was set to 6.25 because it shows to be the more efficient after random experiments according to maximum of the sum of the similarity over all value $\sum \log p(I_F, I_M)$. We neglected the log-term over the Mahalanobis distance in the similarity measure because computation problems occurs with the covariance determinant $|\Sigma|$, so our log likelihood function to maximize becomes :

$$
\log\ p(I_F, I_M) = -\frac{1}{2}(I_F - \mu_{I_M}^*)^t \Sigma^{-1}(I_F - \mu_{I_M}^*) \tag{11}
$$

This result in more stable similarity during the registration. The $\mathcal{GP}$ interpolator was compared to a nearest-neighbour (NN) and spline (SPL) interpolator. Fig. 5 shows the fixed image and the tranformed moving image with the good transformation without interpolation. The pixels don't have the same intensities because they are not in the same physical position, that is why it is important to resample the moving image to compute an exact similarity. After the resampling of the trasnformed moving grid $T(\Omega_{I_M})$, pixels has the same position as in fixed image. We see in Fig. 6 that some patterns appears in resampled images that was not there in original transformed image. $\mathcal{GP}$ is lighter than the other images and the borders (mostly the optic trax) are more clear than other interpolations. The falx of the brain does not appear in the transformed moving image, but it is more distinguishable with $\mathcal{GP}$.

For qualitative results, we computed the mean Target Registration Error (mTRE) respect to the truth transformation [2]. We projected the moving point us-

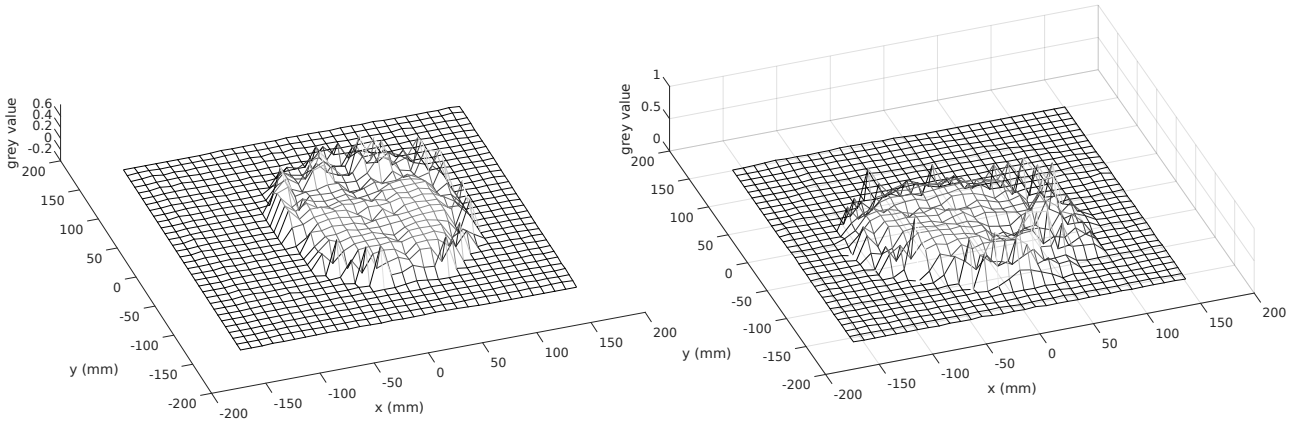

Figure 3. (Left) Grid of fixed image. (Right) Grid of moving image with rotation $\theta = -126.05°$.

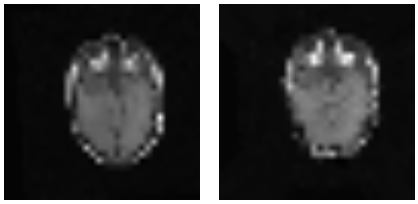

Figure 5. (Left) Fixed image. (Right) Transformed moving image.

Figure 6. (From left to right) Resampled images with respectively NN, SPL and $\mathcal{GP}$ interpolation.

ing the truth transformation and the estimated transformation, then we computed the euclidean distance between all transformed query points. We maximized the similarity measure of eq. 11 for $\mathcal{GP}$ registration and minimized the sum-squared distance (SSD) between the two images for NN and SPL. Fig. 7 shows boxplots and bar plots of the three methods over 100 random transformations and slices. The new similarity measure improve the results about $\sim 15\%$ over the other similarity measure.

We investigated more closely one rigid transformation with a rotation $\theta = -126.05°$ for the moving image. Looking at the cost function of $\mathcal{GP}$, we see that it is thinner than NN or SPL (Fig. 8). Also, a regular patterns appears every modulo of $(\frac{\pi}{2})$, this is due to

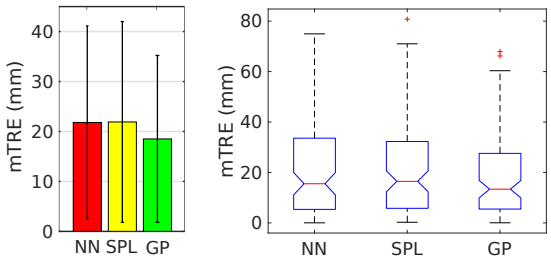

Figure 7. Boxplots and bar plots of the mTRE for the NN, SPL and $\mathcal{GP}$.

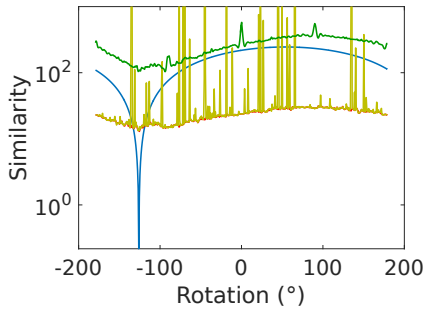

Figure 8. Cost functions for respectively the mTRE (blue), SSD with NN (red), SSD with SPL (yellow) and $\mathcal{GP}$ (green) with the true transformation $-126.05°$ in red.
NOTA : For better evaluation, $-\log p(I_F, I_M)$ was plotted instead of $\log p(I_F, I_M)$ for $\mathcal{GP}$

the influence of the rotation on the grid alignment (see sec. 3.3). Because the spline interpolation is more sensible to noise, some values explode. In the other hand SSD with NN is more stable but the minimum is not clear.

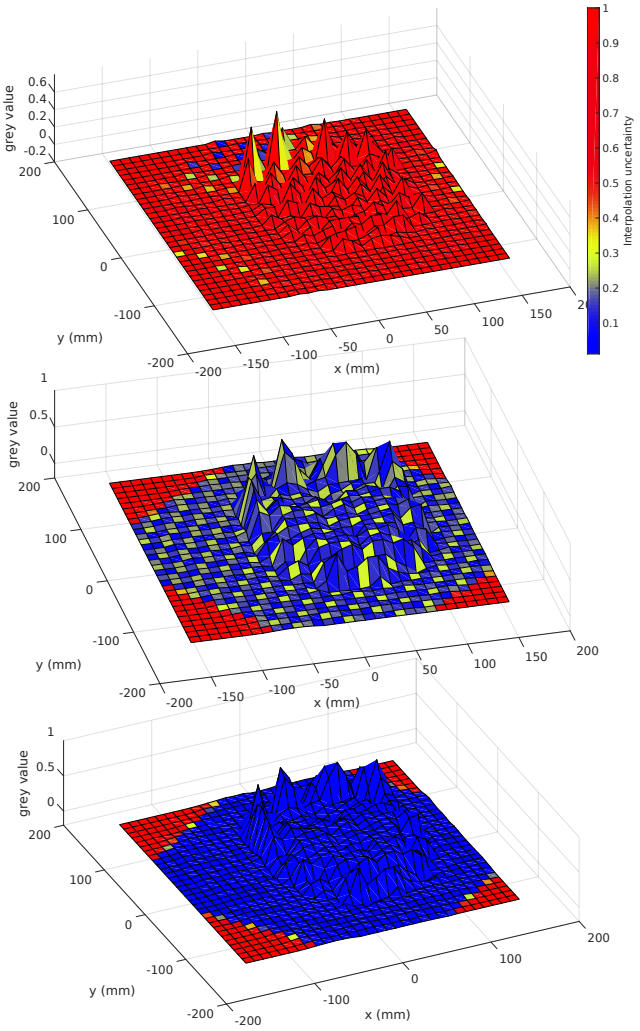

Figure 9. (From top to bottom) Resampling of transformed moving image for $l = 2.5$, $l = 6.25$ and $l = 8$.

3.3. Influence of the parameters

The choice of the lengthscale parameter l for the covariance kernel is one of the most important design in a Gaussian Process. It directly impact the posterior function and consequently the registration of the images. Looking at the Fig. 9, we see that the increasing of l result in the smoothness of the pixel values and diminution of the uncertainty interpolation. This can be explained with the exponential kernel, if l increase the gaussian is wider and there is less variability between the values.

Rotation has an impact on the interpolation uncertainty. Indeed, every modulo of $(\frac{\pi}{2})$ the transformed moving grid X is perfectly aligned with the fixed grid X^* resulting in a null uncertainty (Fig. 10). If the transformation is close to modulo $(\frac{\pi}{4})$, then the uncertainty is maximum and the mTRE will increase.

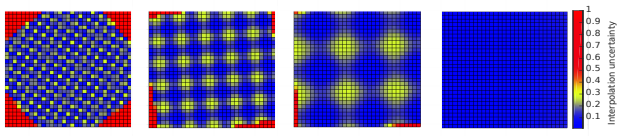

Figure 10. (From left to right) Interpolation uncertainty image with an increasing θ from $(\frac{\pi}{4})$ to $(\frac{\pi}{2})$

4. Conclusion

A new interpolation method for image registration was discussed throughout this paper. Uncertainty varies among points of the resampled moving grid and has to be integrated into the similarity measure which compare the fixed grid and resampled moving grid. Qualitative results shows an improvement of the resampled image compare to nearest-neighbour and spline interpolation. $\mathcal{GP}$ interpolation is more accurate than other and estimate the uncertainty of the interpolation, which allowed the creation of a new generative model for registration with an error reduction of $\sim 15\%$ over the traditional sum of squared differences. The reader must be aware that the computation is more complex than other method and require more memory because of the covariance function construction. Consequently, an image splitting into different blocks is preconized [14]. The covariance function is more sensible to high dimensionality of the problem, moreover distant points tends to be zero which is problematic for the numerical implementation.

Future work will concentrate on choosing the right kernel for the $\mathcal{GP}$ and including translational component into the registration. We did not focus on the optimization method, but a global optimization method like a genetic algorithm [8] can be applied to obtain finer results. Because interpolation increase the resolution of an image using the information of neighbouring observations, a markov random field can be well suited to interpolate values [6].

References

[1] P. Aljabar, J. V. Hajnal, R. G. Boyes, and D. Rueckert. Interpolation artefacts in non-rigid registration. In *Medical Image Computing and Computer-Assisted Intervention–MICCAI 2005*, pages 247–254. Springer, 2005.

[2] E. B. De Kraats, G. P. Penney, D. Tomaževič, T. Van Walsum, and W. J. Niessen. Standardized evaluation methodology for 2-d-3-d registration. *Medical Imaging, IEEE Transactions on*, 24(9):1177–1189, 2005.

[3] J. M. Fitzpatrick, J. B. West, and C. R. Maurer Jr. Predicting error in rigid-body point-based registration. *Medical Imaging, IEEE Transactions on*, 17(5):694–702, 1998.

[4] D. L. Hill, P. G. Batchelor, M. Holden, and D. J. Hawkes. Medical image registration. *Physics in medicine and biology*, 46(3):R1, 2001.

[5] H. S. Hou and H. Andrews. Cubic splines for image interpolation and digital filtering. *Acoustics, Speech and Signal Processing, IEEE Transactions on*, 26(6):508–517, 1978.

[6] M. Li and T. Q. Nguyen. Markov random field model-based edge-directed image interpolation. *Image Processing, IEEE Transactions on*, 17(7):1121–1128, 2008.

[7] P. C. Mahalanobis. On the generalized distance in statistics. *Proceedings of the National Institute of Sciences (Calcutta)*, 2:49–55, 1936.

[8] M. Mitchell. *An introduction to genetic algorithms*. MIT press, 1998.

[9] J. A. Parker, R. V. Kenyon, and D. E. Troxel. Comparison of interpolating methods for image resampling. *Medical Imaging, IEEE Transactions on*, 2(1):31–39, 1983.

[10] C. E. Rasmussen. Gaussian processes for machine learning. 2006.

[11] M. R. Stytz and R. W. Parrott. Using kriging for 3d medical imaging. *Computerized Medical Imaging and Graphics*, 17(6):421–442, 1993.

[12] R. Szeliski and J. Coughlan. Spline-based image registration. *International Journal of Computer Vision*, 22(3):199–218, 1997.

[13] P. Thévenaz, T. Blu, and M. Unser. Image interpolation and resampling. *Handbook of medical imaging, processing and analysis*, pages 393–420, 2000.

[14] C. Wachinger, P. Golland, M. Reuter, and W. Wells. Gaussian process interpolation for uncertainty estimation in image registration. In *Medical Image Computing and Computer-Assisted Intervention–MICCAI 2014*, pages 267–274. Springer, 2014.